ParCFD2024
35^{th} International Conference on Parallel Computational Fluid Dynamics
Sep 02-04 2024, Bonn, Germany

ROADMAP FOR EXTREME-SCALE SIMULATIONS: ON THE EVOLUTION OF POISSON SOLVERS

F.Xavier Trias[1], Àdel Alsalti-Baldellou[1,2] and Assensi Oliva[1]

[1] Heat and Mass Transfer Technological Center, Technical University of Catalonia, C/Colom 11, 08222 Terrassa (Barcelona), francesc.xavier.trias@upc.edu

[2] Department ICEA, University of Padova, Via Francesco Marzolo, 9, 35131 Padova PD, Italy

Key words: Poisson's equation, turbulence, large-scale simulations, DNS, linear solvers

Abstract. We aim to answer the following question: *is the complexity of numerically solving Poisson's equation increasing or decreasing for very large DNS and LES simulations of incompressible flows?* Physical and numerical arguments are combined to derive power-law scalings at very high Reynolds numbers. Theoretical convergence analysis for both Jacobi and multigrid solvers defines a two-dimensional phase space divided into two regions depending whether the number of solver iterations tend to decrease or increase with the Reynolds number. Numerical results seem to confirm that we are in the latter region: *i.e.* in the foreseeable future the numerical complexity of solving Poisson's equation will increase and, therefore, better and better preconditioning techniques will be needed.

1 INTRODUCTION: TWO COMPETING EFFECTS

The never-ending increasing capacity of modern HPC systems enables DNS simulations at higher and higher Reynolds numbers, $Re = Ul/\nu$. The number of grid points, N_x, and time-steps, N_t, can be estimated with the classical Kolmogorov theory (K41)

$$N_x^{K41} = \frac{L_x}{\Delta x} \sim \frac{l}{\eta} \sim Re^{3/4} \qquad N_t^{K41} = \frac{t_{\rm sim}}{\Delta t} \sim \frac{t_l}{t_\eta} \sim \frac{l}{\eta}\frac{u}{U} \sim Re^{3/4} Re^{-1/4} = Re^{1/2}, \quad (1)$$

where L_x and $t_{\rm sim}$ are the domain size and the time integration period, which are assumed to be similar to the size of the largest scales, l, and its corresponding characteristic time, $t_l \sim l/U$, *i.e.* $L_x \sim l$ and $t_{\rm sim} \sim t_l$. For a DNS, we assume that $\Delta x \sim \eta$ and $\Delta t \sim t_\eta \sim \eta/u$, where $t_\eta \sim \eta/u$ and u are the characteristic time and velocity of the Kolmogorov scales, η. Plugging this into the CFL condition, *i.e.* $\Delta t^{\rm conv} \sim \Delta x/U$ and $\Delta t^{\rm diff} \sim \Delta x^2/\nu$ leads to

$$N_t^{\rm conv} \sim \frac{t_l}{\Delta t^{\rm conv}} \sim \frac{l}{U}\frac{U}{lRe^{-3/4}} = Re^{3/4} \qquad N_t^{\rm diff} \sim \frac{t_l}{\Delta t^{\rm diff}} \sim \frac{l}{U}\frac{\nu}{l^2(Re^{-3/4})^2} = Re^{1/2}. \quad (2)$$

Therefore, we can conclude that

$$\Delta t/t_l \sim 1/N_t \sim Re^{\alpha}, \quad (3)$$

where $\alpha = -1/2$ for the K41 theory (see Eq. 1) or diffusion dominated (see Eq. 2, right), and $\alpha = -3/4$ for convection dominated (see Eq. 2, left). Therefore, higher Re lead to

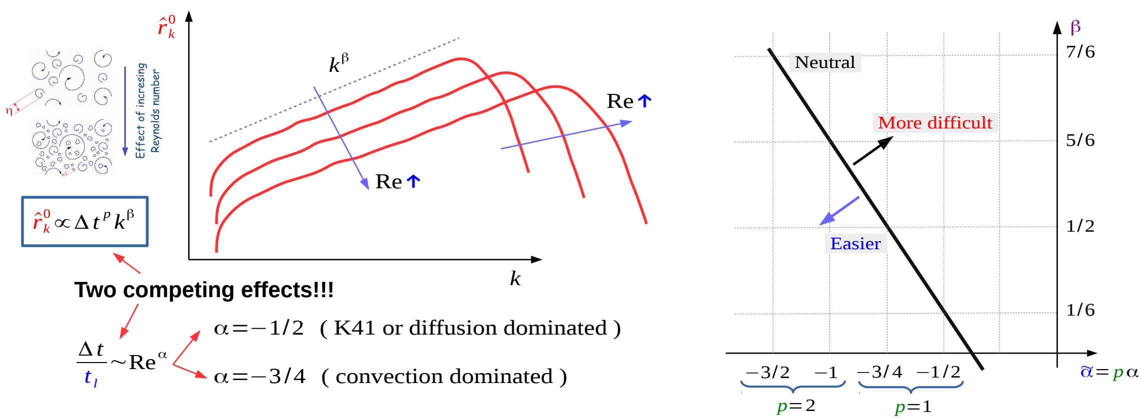

Figure 1: Left: illustrative explanation of the two competing effects on the solution of Poisson's equation when increasing Re number: time-step, Δt, decreases whereas the range of scales increases. Right: $\{\tilde{\alpha}, \beta\}$ phase space. Solid black line corresponds to $\propto Re^0$ in Eqs.(15) and (16), *i.e.* neutral effect of Re-number in the total number of iterations.

(i) larger meshes and (ii) smaller time-steps, Δt. These are two competing effects on the convergence of Poisson's equation: namely, the former increases the condition number of the discrete Poisson equation whereas the latter leads to better initial guess. *Who is eventually the winner at very high Re? Read on...*

2 ANALYSIS OF THE RESIDUAL OF POISSON'S EQUATION

Although FFT-based direct solvers are very well-suited for canonical flows with periodic directions [1], the forthcoming analysis assumes that multigrid (MG) methods will eventually be the preferred option for extreme-scale simulations. Then, the next step is to analyze the residual of the Poisson's equation as a function of the Reynolds number. Relevant aspects are twofold: the magnitude and the spectral distribution. To study them, we consider a fractional step method where $\boldsymbol{u}^p$ is the predictor velocity. Imposing that $\nabla \cdot \boldsymbol{u}^{n+1} = 0$, leads to a Poisson equation for pressure, p^{n+1},

$$\boldsymbol{u}^{n+1} = \boldsymbol{u}^p - \Delta t \nabla p^{n+1} \quad \stackrel{\nabla \cdot}{\Longrightarrow} \quad \nabla^2 p^{n+1} = 1/\Delta t \nabla \cdot \boldsymbol{u}^p. \tag{4}$$

Assuming $\nabla \cdot \boldsymbol{u}^n = 0$ and taking p^n as initial guess, we obtain the following initial residual

$$r^0 = \nabla^2 p^n - \frac{1}{\Delta t} \nabla \cdot \boldsymbol{u}^{p,n+1} \stackrel{(4)}{=} 1/\Delta t \left(\nabla \cdot \boldsymbol{u}^{p,n} - \nabla \cdot \boldsymbol{u}^{p,n+1} \right) \approx \partial_t \nabla \cdot \boldsymbol{u}^p. \tag{5}$$

Alternatively, we can also consider $\tilde{r}^0 = \Delta t r^0$. In this case, the residual reads

$$\tilde{r}^0 = \nabla^2 \tilde{p}^n - \nabla \cdot \boldsymbol{u}^{p,n+1} \stackrel{(4)}{=} \left(\nabla \cdot \boldsymbol{u}^{p,n} - \nabla \cdot \boldsymbol{u}^{p,n+1} \right) \approx \Delta t \partial_t \nabla \cdot \boldsymbol{u}^p, \tag{6}$$

where $\tilde{p} = p\Delta t$ is a pseudo-pressure. Notice that the second residual, $\tilde{r}^0$, is more meaningful from a physical point-of-view, since it directly translates how accurately we impose the incompressibility constraint. Then, recalling that $\nabla \cdot \boldsymbol{u}^p$ can be expressed as follows [2]

$$\nabla \cdot \boldsymbol{u}^p \approx \Delta t \nabla \cdot (\boldsymbol{u} \cdot \nabla \boldsymbol{u}) = 2\Delta t Q_{\mathsf{G}}, \tag{7}$$

leads to

$$r^0 \approx 2\Delta t\ \partial_t Q_{\mathsf{G}} \qquad \text{and} \qquad \tilde{r}^0 \approx 2\Delta t^2 \partial_t Q_{\mathsf{G}}, \tag{8}$$

where $Q_G = -1/2tr(\mathsf{G}^2)$ is the second invariant of the velocity gradient, $\mathsf{G} \equiv \nabla \boldsymbol{u}$. Therefore, smaller Δt decrease the magnitude of r^0 (also $\tilde{r}^0$) leading to a better convergence.

On the other hand, increasing Re also leads to finer meshes (see Eq. 1) and, therefore, to more ill-conditioned systems with a wider and wider range of scales to be resolved. In the forthcoming analysis, the spectral distribution of the initial residual, $\hat{r}^0_k$, plays a crucial role. In general, we can assume a power-law scaling within the inertial range

$$\partial_t Q_{\mathsf{G}} \propto k^{\beta} \qquad \Longrightarrow \qquad \hat{r}^0_k \propto \Delta t^p k^{\beta}, \tag{9}$$

where k is the wavenumber and $p \in \{1, 2\}$ depends on the definition of the residual: $p = 1$ for Eq. (5) and $p = 2$ for Eq. (6). Then, a power-law scaling for Q_{G} can be derived from Eqs.(4) and (7), and the $k^{-7/3}$ scaling of the shell-summed squared pressure spectrum [3],

$$(\hat{Q}_{\mathsf{G}})_k \propto k^2 (k^{-7/3})^{1/2} = k^{5/6}. \tag{10}$$

Then, the value of β in Eq.(9) can be estimated from the dynamics of the invariants obtained from the so-called restricted Euler equations [4],

$$\partial_t Q_{\mathsf{G}} = -(\boldsymbol{u} \cdot \nabla) Q_{\mathsf{G}} - 3R_{\mathsf{G}}, \tag{11}$$

where $R_{\mathsf{G}} = det(\mathsf{G}) = 1/3tr(\mathsf{G}^3)$ is the third invariant of G. The two terms in the right-hand-side of this equation are expected to have different power-law scalings. Namely,

$$(\widehat{(\boldsymbol{u} \cdot \nabla) Q_{\mathsf{G}}})_k \propto (\widehat{\nabla Q_{\mathsf{G}}})_k \propto k(k^{5/6}) = k^{11/6} \qquad \text{and} \qquad (\hat{R}_{\mathsf{G}})_k \propto (k^{5/6})^{3/2} = k^{5/4}, \tag{12}$$

where the Taylor's frozen-turbulence hypothesis is applied to approximate $(\boldsymbol{u} \cdot \nabla) Q_{\mathsf{G}}$, which is eventually the dominant term in the right-hand-side of Eq.(11). Combining this with the results obtained in Eqs.(9) and (12) leads to

$$\boxed{\hat{r}^0_k \propto \Delta t^p k^{\beta} \qquad \text{with} \qquad \beta = 11/6 \quad \text{and} \quad p = \begin{cases} 1 & \text{if } \hat{r} \text{ defined as Eq.(5)} \\ 2 & \text{if } \hat{r} \text{ defined as Eq.(6)} \end{cases}} \tag{13}$$

In summary, there are two competing effects (see Figure 1, left) when increasing Re number: time-step, Δt, decreases whereas the range of scales increases.

3 ANALYSIS OF THE SOLVER CONVERGENCE AND CONCLUSIONS

We can relate the L2-norm of the residual with the integral of $\hat{r}_k$ for all the wavenumbers using the Parseval's theorem, *i.e.* $||r||^2 = \int_\Omega r^2 dV = \int_1^{k_{\max}} \hat{r}_k^2 dk$, where $k_{\max} \approx 1/\eta \sim Re^{3/4}$. Then, the residual after n iterations can be computed as

$$||r^n||^2 = \int_1^{k_{\max}} \left(\hat{\omega}^n_k \hat{r}^0_k\right)^2 dk \overset{(3)(13)}{\approx} \int_1^{Re^{3/4}} \hat{\omega}^{2n}_k Re^{2\tilde{\alpha}} k^{2\beta} dk, \tag{14}$$

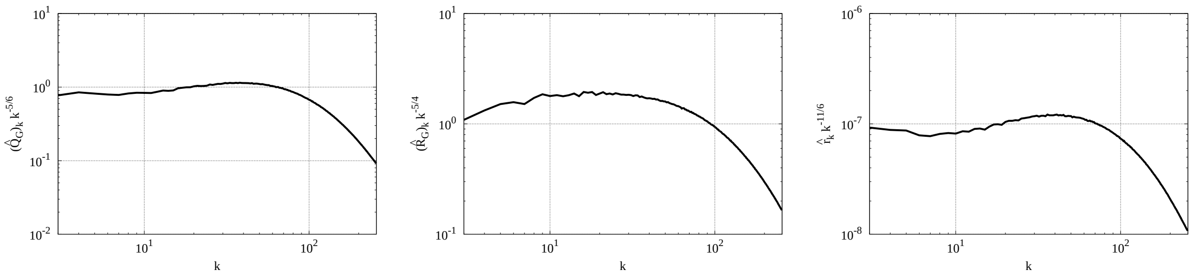

Figure 2: Compensated spectra for pressure, Q_{G}, R_{G}, and the initial solver residual, r_o. Results correspond to forced homogeneous isotropic turbulence at $Re_\lambda = 325$.

where $\hat{\omega}_k = \hat{r}_k^{n+1}/\hat{r}_k^n$ is the convergence ratio of the solver and $\tilde{\alpha} = p\alpha$. For instance, for a Jacobi solver, $\hat{\omega}_k = \cos(\frac{\pi}{2}\rho)$ where $\rho \equiv k/k_{\max}$. In this case, using a quadratic approximation of $\cos(x) \approx 1 - 4x^2/\pi^2$ leads to

$$||r^n||^2 \approx \frac{Re^{2(\tilde{\alpha}+3/4(\beta+1/2))}}{2(2n+1)}. \tag{15}$$

We can extend this analysis for a MG solver with the Jacobi smoother

$$||r^n||^2 \approx \frac{Re^{2(\tilde{\alpha}+3/4(\beta+1/2))}}{2(2n+1)} \left\{ \left(\sum_{l=0}^{l_{\max}} \frac{(3/4)^{2n+1}}{2^{2l}} \right) + \frac{1}{2^{2l_{\max}+1}} \right\}. \tag{16}$$

where $l_{\max} \sim \log_2 N_x \sim (3/4)\log_2 Re$ is the number of levels. Compared to Eq.(15), MG is strongly accelerated by the term in brackets, which tends to $(3/4)^{2n}$. Nevertheless, the Re-scaling is the same; therefore, the regions defined in the $\{\tilde{\alpha}, \beta\}$ phase space remain unchanged (see Figure 1, right). Numerical results displayed in Figure 2 seem to confirm our theory: namely, the slopes of the invariants Q_{G} and R_{G} correspond well with the values predicted in Eqs.(10) and (12), respectively. More importantly, the slope of the solver residual, $\hat{r}_k$, fits with the predicted value of $\beta = 11/6$ (see Eq.13). Altogether leads to the preliminary conclusion that the number of iterations tends to increase with Re.

Acknowledgements

This work was financially supported by the SIMEX project (PID2022-142174OB-I00) of *Ministerio de Ciencia e Innovación*, Spain. Calculations were carried out on the MareNostrum 4 supercomputer at BSC. We thankfully acknowledge these institutions.

References

[1] F. X. Trias, M. Soria, C. D. Pérez-Segarra, and A. Oliva. A Direct Schur-Fourier Decomposition for the Efficient Solution of High-Order Poisson Equations on Loosely Coupled Parallel Computers. *Numerical Linear Algebra with Applications*, 13:303–326, 2006.

[2] Stephen B. Pope. *Turbulent Flows*. Cambridge University Press, 2000.

[3] D. I. Pullin. Pressure spectra for vortex models of fine-scale homogeneous turbulence. *Physics of Fluids*, 7:849, 1995.

[4] B. J. Cantwell. Exact solution of a restricted Euler equation for the velocity gradient tensor. *Physics of Fluids A*, 4:782–793, 1992.